

Consistency between ARPES and STM measurements on SmB₆

Christian E. Matt,¹ Harris Pirie,¹ Anjan Soumyanarayanan,¹ Michael M. Yee,¹ Yang He,¹ Daniel T. Larson,¹ Wendel S. Paz,² J.J. Palacios,³ M.H. Hamidian,¹ and Jennifer E. Hoffman¹

¹*Department of Physics, Harvard University, Cambridge, MA, 02138, USA*

²*Instituto de Física, Universidade Federal do Rio de Janeiro, Caixa Postal 68528, Rio de Janeiro, RJ 21941-972, Brazil*

³*Departamento de Física de la Materia Condensada, Condensed Matter Physics Center (IFIMAC) and Instituto Nicolás Cabrera (INC), Universidad Autónoma de Madrid, Cantoblanco, 28049 Madrid, Spain*

(Dated: September 3, 2022)

Strongly correlated topological surface states are promising platforms for next-generation quantum applications, but they remain elusive in real materials. The correlated Kondo insulator SmB₆ is one of the most promising candidates, with theoretically predicted heavy Dirac surface states supported by transport and scanning tunneling microscopy (STM) experiments. However, a puzzling discrepancy appears between STM and angle-resolved photoemission (ARPES) experiments on SmB₆. Although ARPES detects spin-textured surface states, their velocity is an order of magnitude higher than expected, while the Dirac point – the hallmark of any topological system – can only be inferred deep within the bulk valence band. A significant challenge is that SmB₆ lacks a natural cleavage plane, resulting in ordered surface domains limited to 10s of nanometers. Here we use STM to show that surface band bending can shift energy features by 10s of meV between domains. Starting from our STM spectra, we simulate the full spectral function as an average over multiple domains with different surface potentials. Our simulation shows excellent agreement with ARPES data, and thus resolves the apparent discrepancy between large-area measurements that average over multiple band-shifted domains and atomically-resolved measurements within a single domain.

INTRODUCTION

The emergent electronic properties of Kondo insulators are caused by the interaction of itinerant conduction electrons with a magnetic Kondo lattice formed by localized f electrons. [1, 2]. At high temperatures the conduction electrons scatter only weakly at the localized moments but below the Kondo temperature T_K the scattering is strong enough that the conduction electrons hybridize with the f -band, opening a gap at E_F . The resistivity upturn in electrical transport experiments on the canonical Kondo insulator SmB₆ demonstrates the formation of such a hybridization gap below ~ 50 K [3]. However, saturation of the resistivity below 5 K indicates the emergence of an additional conduction channel. Several theoretical studies using complementary approaches based on renormalized band theory and tight binding Hamiltonians matched to LDA (+Gutzwiller) calculations[4–6], have predicted the strong topological insulating nature of SmB₆ and the existence of 3 Dirac cones with heavy quasiparticles on the surface of SmB₆, as shown in Fig. 1. Such low velocity Dirac fermions in SmB₆ produce a high density of states at the Fermi level, increasing their susceptibility to exotic orders and their potential utility for novel technologies.

There has been significant progress in experimentally verifying these exciting predictions. The hybridization gap of the Sm $4f$ and $5d$ band has been observed at low temperatures by scanning tunneling microscopy (STM) [7–11] and also suggested by angle-resolved photoemis-

TABLE I. Comparison of SmB₆ surface state properties predicted by theory and measured by photoemission and STM. We tabulate values for the Fermi velocity v , Dirac point energy E_D , and surface Fermi wavevector k_F at both the \bar{X} and $\bar{\Gamma}$ points of the surface Brillouin zone.

	Theory [6]	Photoemission [19]	STM [20]
$v_{\bar{X}}$ (meV·Å)	16 ± 2	240 ± 20	7.6 ± 0.3
$E_{D_{\bar{X}}}$ (meV)	1 ± 1	-65 ± 4	-5.4 ± 0.1
$2(k_{F_{\bar{X}}} - \bar{X})(\frac{\pi}{a_0})$	0.25 ± 0.02	0.38 ± 0.03	0.54 ± 0.02
$v_{\bar{\Gamma}}$ (meV·Å)	50 ± 2	220 ± 20	90 ± 9
$E_{D_{\bar{\Gamma}}}$ (meV)	-7 ± 1	-23 ± 3	-9 ± 2
$2k_{F_{\bar{\Gamma}}}(\frac{\pi}{a_0})$	0.18 ± 0.02	0.12 ± 0.03	0.07 ± 0.01

sion spectroscopy (ARPES) [12–15]. Further, ARPES experiments have shown spin-textured surface states in the hybridization gap [16, 17]. Unfortunately, the hallmark of a correlated topological state – its Dirac point – has not yet been clearly resolved by ARPES [14], and the surface states reported by ARPES to date are an order of magnitude higher than theoretical predictions, as shown in Table I. This has led to the suggestion that the Dirac point could be pushed down into the valence band by a sufficiently strong band-bending potential [18].

SmB₆ lacks a natural cleavage plane, which leads to surface domain sizes on the order of tens of nanometers as measured by STM [7–11]. On the other hand, the typical photoemission spot size is on the order of tens of microns [21]. Since ARPES measurements report strong spatial variations of the low energy photoemission signal

on macroscopic length scales [12, 22], it is clear that they necessarily average over various domains on the SmB_6 surface. If there is significant polarity-driven band bending that differs between the various domains, ARPES spectra will contain a superposition of spectral features that are shifted in energy with respect to each other.

Here we use STM spectroscopy to guide a simulation of the energy and momentum broadened spectral functions for the Sm-terminated surfaces with the polar 1×1 and non-polar 2×1 reconstruction. We demonstrate that for a range of realistic experimental parameters the in-gap topological surface states will appear in ARPES experiments with artificially enhanced Fermi velocity. Furthermore, our findings provide an explanation for the discrepancy between the electronic band structure measured by ARPES and theoretical predictions.

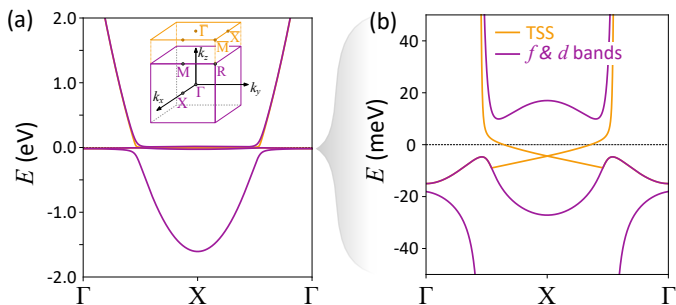


FIG. 1. Schematic representation of the SmB_6 band structure, showing 2 weakly dispersing f -bands and a strongly dispersing d -band, in addition to the Dirac cone of the topological surface state (TSS). Inset of (a): Bulk and surface Brillouin zone (BZ) of SmB_6 .

METHODS

STM experiments were performed on single crystals of SmB_6 grown using the Al-flux method [23]. The crystals were cleaved in cryogenic ultra high vacuum at ~ 30 K and then inserted into the STM head. STM tips are prepared by *in situ* field emission on Au foil.

Our calculations were performed in the framework of density functional theory (DFT), as implemented in the Quantum ESPRESSO package [24]. The generalized gradient approximation of Perdew-Burke-Ernzerhof (GGA-PBE) [25] was adopted for the exchange-correlation functional. The electron-ion interactions are described using ultrasoft pseudopotentials with valence electron configurations of $2s^2 2p^1$ for B atoms and $5s^2 4d^{10} 5p^6 6s^2 4f^6$ for Sm atoms. The energy cutoff for the plane wave basis is 120 Ry with a charge density cutoff of 500 Ry. We have used a Monkhorst-Pack [26] scheme with a $12 \times 12 \times 1$ k-mesh for the Brillouin zone integration for the supercell with one unit cell (1×1 Sm) and $6 \times 12 \times 1$ for the supercell with two unit cells (2×1 Sm). In all calculations

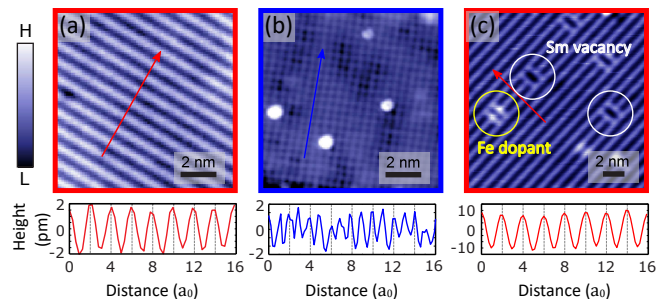


FIG. 2. STM topography of the 1×1 (a) and 2×1 (b) reconstructed Sm terminated SmB_6 surfaces. Setpoints are: (a) $V_s = 200$ mV, $R_J = 10\text{G}\Omega$ and (b) $V_s = 100$ mV, $R_J = 5\text{G}\Omega$. (c) STM image of an Fe dopant located in the bright band of a 2×1 domain.

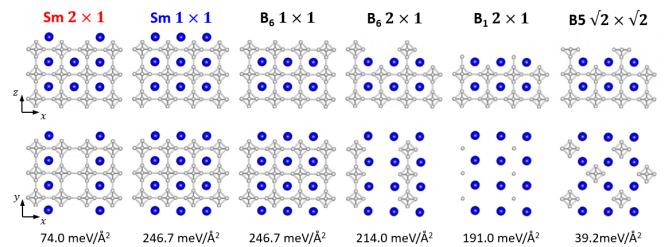


FIG. 3. Top-view (upper) and side-view (lower) of different surface reconstructions and their corresponding surface formation energy.

the lattice parameter was kept fixed at the experimental value $a = 4.13$ Å, with a slab thickness of 25.0 Å and 15 Å of vacuum space to minimize interactions between the periodic images. Neither spin polarization nor spin-orbit coupling were considered since our focus is on the electrostatics of the material.

RESULTS

Surface characterization

Because SmB_6 does not have a natural cleavage plane, different surface terminations are observed. High resolution 10×10 nm STM topographies presented in Fig. 2(a)-(b) show the morphology of two different ordered domains which are common throughout the crystal surface. Fig. 2(a) shows the most prevalent ordered domain structure, a 2×1 reconstructed Sm surface where half of the Sm atoms have been removed during the cleave, with the remaining Sm atoms arranging themselves in a striped pattern. This is consistent with observations of 2×1 reconstructions in LEED [27] and band folding in ARPES [13, 22]. In lightly Fe-doped SmB_6 samples, where Fe atoms replace Sm atoms, the defects are always located on the bright stripes as shown in Fig. 2(c), which further

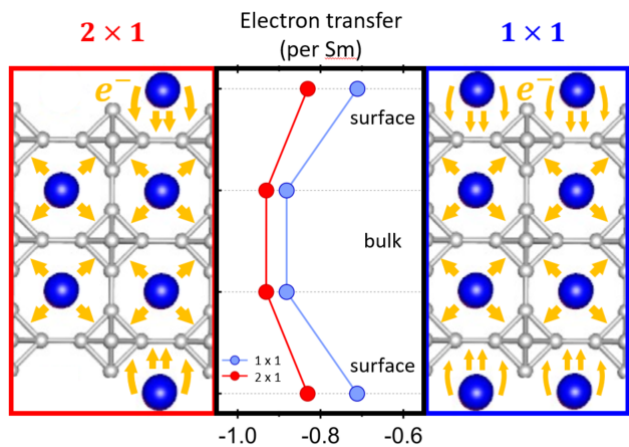


FIG. 4. Distribution of projected atomic charges per Sm atom (Löwdin charges calculated from DFT) illustrating the electron transfer from Sm to B_6 layers for the 2×1 (left panel) and 1×1 (right panel) surfaces. Arrow thickness indicates amount of electrons transferred from each Sm atom into surrounding B_6 clusters. The central panel plots the relative charge transfer. Fewer electrons are drawn from each Sm atom on the 1×1 surface as compared to the 2×1 surface.

confirms that this is indeed the Sm-terminated surface [20]. Another domain structure is the 1×1 square lattice shown in Fig. 2(b) which we identify as a full Sm layer, similar to previous reports on LaB_6 [7, 28].

DFT calculations of the surface formation energy are shown in Fig. 3. The significantly lower formation energy for the 2×1 Sm surface compared to the 1×1 Sm surface matches with the observed preponderance of the former structure. Since terminations with B_5 clusters tend to form disordered regions[11], the lower formation energies for some B terminations are likely responsible for many of the disordered domains that are observed.

Termination-dependent band bending

To better understand the differences in the electronic environment between the 2×1 and 1×1 Sm terminations, we calculated the relative charge transfer from Sm to B_6 layers using Löwdin population analysis to partition the charge[29, 30], with results shown in Fig. 4. For both terminations, the Sm atoms in the surface layers have fewer neighboring B atoms to accept electrons, so will have a slightly lower charged state than their bulk counterparts. This corresponds to increased electron density near the surface and leads to greater filling of the surface Sm orbitals and thus a slight downward bending of the surface bands. This effect is less pronounced in the 2×1 reconstruction due to the absence of half of the Sm atoms on the surface. Thus we expect a downward shift in the DOS of the 1×1 termination relative to the 2×1 termination.

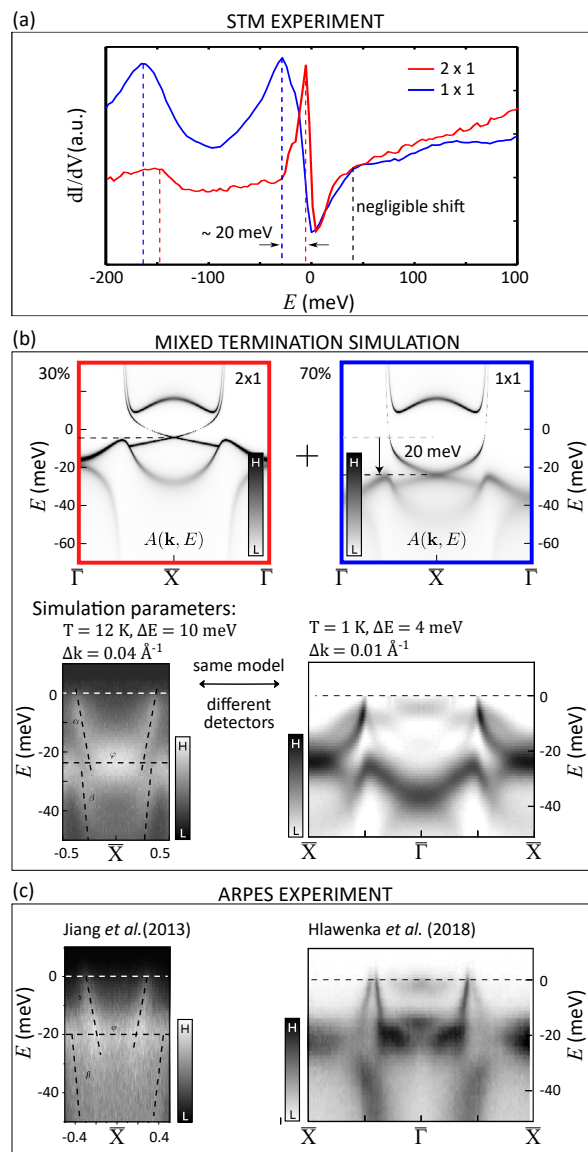


FIG. 5. (a) Measured dI/dV on two different surfaces of SmB_6 . (b) Starting with the electronic structure inferred by STM on the non-polar 2×1 surface (red), we simulate the 1×1 polar termination by rigidly shifting the occupied states down by ~ 20 meV (blue). The average of the simulated spectral function from the 2×1 and 1×1 surface imitates the scenario of a spatially integrating measurement. The averaged spectrum has been convoluted with a Gaussian-shape function in order to account for finite temperature, energy and momentum resolution. Realistic experimental parameters as reported in Refs. [19] and [22] have been used to simulate the spectra along $\bar{M} - \bar{X} - \bar{M}$ and $\bar{X} - \bar{\Gamma} - \bar{X}$ direction. Despite the low-velocity Dirac fermions we started with, both simulations show high-velocity states at the Fermi level that reproduce the ARPES experimental data presented in Refs. [19] and [22]. (c) Two different ARPES intensity maps shown for direct comparison with our mixed-termination simulations in panel (b). Reprinted from [19] and [22].

Figure 5(a) shows the measured differential conduc-

tance, $dI/dV(\mathbf{r}, E) \equiv g(\mathbf{r}, E)$, where I is the tunneling current and V is the bias applied to the sample with respect to the tip. We observe 3 pronounced spectral features: a peak at approximately -150 meV, a peak close to E_F , and a shoulder at ~ 40 meV. Previous STM studies have identified these peaks as Sm $4f$ states based on ARPES and dynamical mean field theory (DMFT) calculations [11, 31]. Below the Fermi energy both peaks of the 1×1 surface are clearly downward shifted by ~ 20 meV with respect to the 2×1 surface, just as expected from the DFT calculations. Interestingly, the shoulders on the unoccupied side of the DOS remain at roughly at the same energies.

Spectral function simulation

The upper plots in Fig. 5(b) show the simulated spectral function of the low energy electronic structure for the 2×1 and 1×1 surface terminations. In both cases the spectral function includes bulk features, namely two weakly dispersing f bands and one strongly dispersing d band, along with the Dirac cone of the topological surface state. The spectral function describes a Fermi liquid-like quasiparticle decay rate $\sim \omega^2$ [32]. The energies of the f - and d -bands are taken from the STM spectra shown in Fig. 5(a). It can be seen that the occupied electronic bands of the 1×1 reconstructed surface are shifted lower by 20 meV compared to the 2×1 surface, while the unoccupied states are not shifted. The lower plots in Fig. 5(b) show the average of the spectral function of both surfaces convoluted with a Gaussian-like function to simulate realistic detector resolution and temperature broadening. The left plot simulates a cut along $\bar{M} - \bar{X} - \bar{M}$ with $T = 12$ K, $\Delta E = 10$ meV $\Delta k = 0.04 \text{\AA}^{-1}$, while the right plot is a cut along $\bar{X} - \bar{\Gamma} - \bar{X}$ with $T = 1$ K, $\Delta E = 4$ meV $\Delta k = 0.01 \text{\AA}^{-1}$. These parameters are chosen to match the conditions in ARPES experiments reported in [19] and [22], which are reproduced in Fig. 5(c). The main features of these ARPES spectra, including the high velocity of the in-gap states and the approximate gap size of 20 meV, are well captured by our simulation.

DISCUSSION

Our STM spectroscopy measurements on the 1×1 surface show a clear downward shift in the differential conductance peaks at negative bias compared to the peaks measured on the 2×1 surface. Such a band-bending scenario is a well understood phenomenon in semiconductors [33], and can be readily understood by appealing to the different amounts of charge transfer predicted by our DFT calculations as shown in Fig. 4.

It has been argued that the polar surfaces in SmB_6 result in topologically trivial surface states [34, 35]. How-

ever, here we provide a different scenario: We observe only a shift of the occupied states between the two surfaces and constant features on the unoccupied side, similar to recent STM result on SmB_6 surfaces with disordered B-clusters which has been interpreted as an increase of the Kondo hybridization gap [11].

To discuss the implications of excess charge on the topologically non-trivial surface it is useful to summarize our results for the 2×1 surface. On the 2×1 surface topologically non-trivial surface states with heavy Dirac fermions and a Dirac point at -5 ± 1 meV has been observed [20]. On the 1×1 surface, due to additional charge, this Dirac point is pushed to lower energies. In our simulation we assumed that the quasiparticle mass at the Dirac point is not changed.

Several different STM studies have all found that single-termination domain sizes are on the order of 10 nm [7–11]. On the other hand, a typical photon beam spot size in an ARPES experiment is roughly $50 \mu\text{m} \times 50 \mu\text{m}$. This implies that ARPES measurements, while potentially favoring certain terminations [21, 22], will still be sensitive to multiple domain types. The averaged spectral function presented in Fig. 5(e) and (f) has been simulated assuming the surface consists of 70% 1×1 domains and 30% 2×1 domains. The resulting intensity plot shows remarkable similarities to reported ARPES measurements with similarly large velocities for the averaged topological surface states. In addition, note that the Dirac point cannot be resolved in the simulation.

CONCLUSION

In summary, our STM spectra show downward band bending on the Sm terminated 1×1 reconstructed surface due to excess charge accumulation as compared to the 2×1 Sm surface, in agreement with our DFT calculations. To study the effect of these different domains we simulated the full spectral function as an average over multiple domains with surfaces potentials and band-bending based on STM measurements. Our simulations show a low energy electronic structure with large band velocities and no resolvable Dirac cone. This provides a likely explanation for the discrepancy between ARPES measurements, which sample multiple domains, and STM measurements taken within a single domain.

ACKNOWLEDGEMENTS

We thank Zachary Fisk and Dae-Jeong Kim for providing the samples. Experiments were supported by National Science Foundation DMR-1410480. HP and MHH were funded by the Gordon and Betty Moore Foundations EPiQS Initiative through Grant GBMF4536. CEM is supported by the Swiss National Science Foundation

under fellowships P2EZP2.175155. JJP and WP acknowledge Sahar Pakdel for her contribution at the initial stages of this work and financial support from Spanish MINECO through Grant FIS2016-80434-P, the Fundación Ramn Areces, the María de Maeztu Program for Units of Excellence in R&D (MDM-2014-0377), the Comunidad Autónoma de Madrid through MAD2D-CM Program (S2013/MIT-3007), and the European Union Seventh Framework Programme under Grant agreement No. 604391 Graphene Flagship. WP was funded by the CNPq Fellowship programme (Pós-doutorado júnior) under grant 405107/2017-0 and acknowledges the computer resources and assistance provided by the Centro de Computación Científica of the Universidad Autónoma de Madrid and the RES.

-
- [1] Maxim Dzero, Jing Xia, Victor Galitski, and Piers Coleman, “Topological Kondo insulators,” *Annual Review of Condensed Matter Physics* **7**, 249–280 (2016).
- [2] Prasanta Misra, “Handbook of metal physics: Heavy-fermion systems,” **2**, 291–333 (2009).
- [3] D. J. Kim, J. Xia, and Z. Fisk, “Topological surface state in the Kondo insulator samarium hexaboride,” *Nature Materials* **13**, 466–470 (2014).
- [4] Maxim Dzero, Kai Sun, Victor Galitski, and Piers Coleman, “Topological Kondo insulators,” *Physical Review Letters* **104**, 106408 (2010).
- [5] Victor Alexandrov, Maxim Dzero, and Piers Coleman, “Cubic topological Kondo insulators,” *Physical review letters* **111**, 226403 (2013).
- [6] Feng Lu, JianZhou Zhao, Hongming Weng, Zhong Fang, and Xi Dai, “Correlated topological insulators with mixed valence,” *Physical Review Letters* **110**, 096401 (2013).
- [7] Michael M. Yee, Yang He, Anjan Soumyanarayanan, Dae-Jeong Kim, Zachary Fisk, and Jennifer E. Hoffman, “Imaging the Kondo insulating gap on SmB_6 ,” arXiv:1308.1085 [cond-mat] (2013), arXiv:1308.1085 [cond-mat].
- [8] Wei Ruan, Cun Ye, Minghua Guo, Fei Chen, Xianhui Chen, Guang-Ming Zhang, and Yayu Wang, “Emergence of a coherent in-gap state in the Kondo insulator revealed by scanning tunneling spectroscopy,” *Physical Review Letters* **112**, 136401 (2014).
- [9] Sahana Rößler, Tae-Hwan Jang, Dae-Jeong Kim, L. H. Tjeng, Zachary Fisk, Frank Steglich, and Steffen Wirth, “Hybridization gap and fano resonance in SmB_6 ,” *Proceedings of the National Academy of Sciences* **111**, 4798–4802 (2014).
- [10] L. Jiao, S. Rößler, D J Kim, L H Tjeng, Z Fisk, F Steglich, and S Wirth, “Additional energy scale in SmB_6 at low-temperature, volume = 7, year = 2016,” *Nature Communications*, 13762.
- [11] Zhixiang Sun, Ana Maldonado, Wendel S. Paz, Dmytro S. Inosov, Andreas P. Schnyder, J. J. Palacios, Natalya Yu. Shitsevalova, Vladimir B. Filipov, and Peter Wahl, “Observation of a well-defined hybridization gap and in-gap states on the SmB_6 (001) surface,” *Physical Review B* **97**, 235107 (2018).
- [12] Jonathan D. Denlinger, James W. Allen, Jeong-Soo Kang, Kai Sun, Byung-II Min, Dae-Jeong Kim, and Zachary Fisk, “ SmB_6 photoemission: Past and present,” in *Proceedings of the International Conference on Strongly Correlated Electron Systems (SCES2013)*, JPS Conference Proceedings, Vol. 3 (Journal of the Physical Society of Japan, 2014).
- [13] N. Xu, X. Shi, P. K. Biswas, C. E. Matt, R. S. Dhaka, Y. Huang, N. C. Plumb, M. Radović, J. H. Dil, E. Pomjakushina, K. Conder, A. Amato, Z. Salman, D. McK. Paul, J. Mesot, H. Ding, and M. Shi, “Surface and bulk electronic structure of the strongly correlated system smb_6 and implications for a topological Kondo insulator,” *Physical Review B* **88**, 121102 (2013).
- [14] N. Xu, C. E. Matt, E. Pomjakushina, X. Shi, R. S. Dhaka, N. C. Plumb, M. Radović, P. K. Biswas, D. Evtushinsky, V. Zabolotnyy, J. H. Dil, K. Conder, J. Mesot, H. Ding, and M. Shi, “Exotic Kondo crossover in a wide temperature region in the topological Kondo insulator SmB_6 revealed by high-resolution ARPES,” *Physical Review B* **90**, 085148 (2014).
- [15] M. Neupane, N. Alidoust, S.-Y. Xu, T. Kondo, Y. Ishida, D. J. Kim, Chang Liu, I. Belopolski, Y. J. Jo, T.-R. Chang, H.-T. Jeng, T. Durakiewicz, L. Balicas, H. Lin, A. Bansil, S. Shin, Z. Fisk, and M. Z. Hasan, “Surface electronic structure of the topological Kondo-insulator candidate correlated electron system $\text{smb}_{\text{sub}z}6_{\text{sub}z}$,” *Nature Communications* **4**, 2991 (2013).
- [16] N. Xu, P. K. Biswas, J. H. Dil, R. S. Dhaka, G. Landolt, S. Muff, C. E. Matt, X. Shi, N. C. Plumb, M. Radović, E. Pomjakushina, K. Conder, A. Amato, S. V. Borisenko, R. Yu, H.-M. Weng, Z. Fang, X. Dai, J. Mesot, H. Ding, and M. Shi, “Direct observation of the spin texture in SmB_6 as evidence of the topological Kondo insulator,” *Nature Communications* **5**, 4566 (2014).
- [17] Shigemasa Suga, Kazuyuki Sakamoto, Taichi Okuda, Koji Miyamoto, Kenta Kuroda, Akira Sekiyama, Junichi Yamaguchi, Hidenori Fujiwara, Akinori Irizawa, Takahiro Ito, Shinichi Kimura, T. Balashov, W. Wulfhekel, S. Yeo, Fumitoshi Iga, and Shin Imada, “Spin-polarized angle-resolved photoelectron spectroscopy of the so-predicted Kondo topological insulator SmB_6 ,” *Journal of the Physical Society of Japan* **83**, 014705 (2013).
- [18] Bitan Roy, Jay D Sau, Maxim Dzero, and Victor Galitski, “Surface theory of a family of topological Kondo insulators,” *Physical Review B* **90**, 155314 (2014).
- [19] J. Jiang, S. Li, T. Zhang, Z. Sun, F. Chen, Z. R. Ye, M. Xu, Q. Q. Ge, S. Y. Tan, X. H. Niu, M. Xia, B. P. Xie, Y. F. Li, X. H. Chen, H. H. Wen, and D. L. Feng, “Observation of possible topological in-gap surface states in the Kondo insulator $\text{smb}_{\text{sub}z}6_{\text{sub}z}$ by photoemission,” *Nature Communications* **4**, 3010 (2013).
- [20] Harris Pirie, Yu Liu, A. Soumyanarayanan, Pengcheng Chen, Yang He, M.M. Yee, P.F.S. Rosa, J.D. Thompson, Dae-Jeong Kim, Z. Fisk, Xiangfeng Wang, J. Paglione, Dirk K. Morr, M.H. Hamidian, and Jennifer E. Hoffman, “Imaging emergent heavy Dirac fermions of a topological Kondo insulator,” (2018).
- [21] Nan Xu, Hong Ding, and Ming Shi, “Spin- and angle-resolved photoemission on the topological Kondo insulator candidate: SmB_6 ,” *Journal of Physics: Condensed Matter* **28**, 363001 (2016).

- [22] P. Hlawenka, K. Siemensmeyer, E. Weschke, A. Varykhalov, J. Sánchez-Barriga, N. Y. Shitsevalova, A. V. Dukhnenko, V. B. Filipov, S. Gabáni, K. Flachbart, O. Rader, and E. D. L. Rienks, “Samarium hexaboride is a trivial surface conductor,” *Nature Communications* **9**, 517 (2018).
- [23] D. J. Kim, S. Thomas, T. Grant, J. Botimer, Z. Fisk, and Jing Xia, “Surface hall effect and nonlocal transport in SmB_6 : Evidence for surface conduction,” *Scientific Reports* **3**, 3150 (2013).
- [24] Paolo Giannozzi, Stefano Baroni, Nicola Bonini, Matteo Calandra, Roberto Car, Carlo Cavazzoni, Davide Ceresoli, Guido L. Chiarotti, Matteo Cococcioni, Ismaila Dabo, Andrea Dal Corso, Stefano de Gironcoli, Stefano Fabris, Guido Fratesi, Ralph Gebauer, Uwe Gerstmann, Christos Gougoussis, Anton Kokalj, Michele Lazzeri, Layla Martin-Samos, Nicola Marzari, Francesco Mauri, Riccardo Mazzarello, Stefano Paolini, Alfredo Pasquarello, Lorenzo Paulatto, Carlo Sbraccia, Sandro Scandolo, Gabriele Sclauzero, Ari P. Seitsonen, Alexander Smogunov, Paolo Umari, and Renata M. Wentzcovitch, “QUANTUM ESPRESSO: A modular and open-source software project for quantum simulations of materials,” *Journal of Physics: Condensed Matter* **21**, 395502 (2009).
- [25] John P. Perdew, Kieron Burke, and Matthias Ernzerhof, “Generalized gradient approximation made simple,” *Physical Review Letters* **77**, 3865–3868 (1996).
- [26] Hendrik J Monkhorst and James D Pack, “Special points for brillouin-zone integrations,” *Physical review B* **13**, 5188 (1976).
- [27] Hidetoshi Miyazaki, Tetsuya Hajiri, Takahiro Ito, Satoru Kunii, and Shin-ichi Kimura, “Momentum-dependent hybridization gap and dispersive in-gap state of the Kondo semiconductor SmB_6 ,” *Physical Review B* **86**, 075105 (2012).
- [28] John S. Ozcomert and Michael Trenary, “Atomically resolved surface structure of $\text{LaB}_6(100)$,” *Surface Science* **265**, L227–L232 (1992).
- [29] Per-Olov Löwdin, “On the nonorthogonality problem connected with the use of atomic wave functions in the theory of molecules and crystals,” *J. Chem. Phys.* **18**, 365 (1950).
- [30] PO Löwdin, “On the nonorthogonality problem,” *Adv. Quantum Chem.* **5**, 185 (1970).
- [31] J. D. Denlinger, J. W. Allen, J.-S. Kang, K. Sun, J.-W. Kim, J. H. Shim, B. I. Min, Dae-Jeong Kim, and Z. Fisk, “Temperature dependence of linked gap and surface state evolution in the mixed valent topological insulator SmB_6 ,” arXiv:1312.6637 [cond-mat] (2013), arXiv:1312.6637 [cond-mat].
- [32] C. M. Varma, Z. Nussinov, and Wim van Saarloos, “Singular or non-Fermi liquids,” *Physics Reports* **361**, 267–417 (2002).
- [33] Zhen Zhang and John T. Yates, “Band bending in semiconductors: Chemical and physical consequences at surfaces and interfaces,” *Chemical Reviews* **112**, 5520–5551 (2012).
- [34] E. Frantzeskakis, N. de Jong, B. Zwartsenberg, Y. K. Huang, Y. Pan, X. Zhang, J. X. Zhang, F. X. Zhang, L. H. Bao, O. Tegus, A. Varykhalov, A. de Visser, and M. S. Golden, “Kondo hybridization and the origin of metallic states at the (001) surface of SmB_6 ,” *Physical Review X* **3**, 041024 (2013).
- [35] Z.-H. Zhu, A. Nicolaou, G. Levy, N. P. Butch, P. Syers, X. F. Wang, J. Paglione, G. A. Sawatzky, I. S. Elfimov, and A. Damascelli, “Polarity-driven surface metallicity in SmB_6 ,” *Physical Review Letters* **111**, 216402 (2013).